Metallomics

Accepted Manuscript

This article can be cited before page numbers have been issued, to do this please use: B. Gomez-Gomez, L. Arregui, S. Serrano, A. Santos, M. T. Perez-Corona and Y. Madrid, *Metallomics*, 2019, DOI: 10.1039/C9MT00044E.

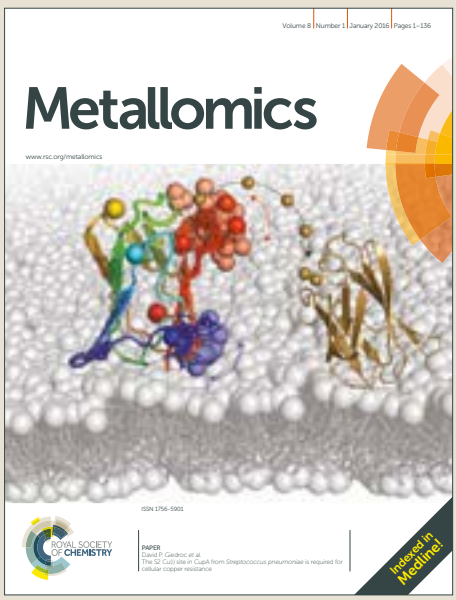

ROYAL SOCIETY OF CHEMISTRY

rsc.li/metallomics

Selenium and tellurium-based nanoparticles as interfering factors on Quorum sensing-regulated processes: violacein production and bacterial biofilm formation.

Beatriz Gómez-Gómez[1], Lucia Arregui[2], Susana Serrano [2], Antonio Santos[2], Teresa Pérez-Corona[1] Yolanda Madrid[1*].

[1] Department of Analytical Chemistry, Faculty of Chemistry, Complutense University of Madrid, Av. Complutense s/n 28040 Madrid, Spain

[2] Department of Genetics, Physiology and Microbiology, Faculty of Biology, Complutense University of Madrid, José Antonio Novais 12, 28040 Madrid, Spain.

*Corresponding Author:
Prof. Yolanda Madrid Albarrán
Dept. of Analytical Chemistry
Faculty of Chemistry
Universidad Complutense de Madrid
E-28040 Madrid, Spain
Phone: ++0034913945145
Fax: ++0034913944329

TABLE OF CONTENTS ENTRY

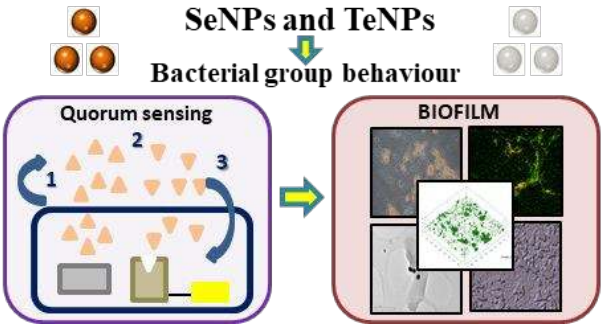

The effect of SeNPs and TeNPs on different process regulated by QS such as violacein production and biofilm formation is presented. The data open new strategies for controlling persistent infections

ABSTRACT

A cell-to-cell communication system called quorum sensing (QS) promotes the transcription of certain target genes in bacterial cells leading to the activation of different cellular processes, some of them related to bacterial biofilm formation. The formation of bacterial biofilm favours antibiotic resistance that is nowadays a significant public-health problem. In this study, the effect of selenium (SeNPs) and tellurium (TeNPs) nanoparticles was examined in two bacterial processes mediated by QS: violacein production by *Chromobacterium violaceum* and biofilm formation by *Pseudomonas aeruginosa*. For this purpose, quantification of the pigment production in presence of these nanoparticles was monitored using the *C. violaceum* strain. Additionally, a combination of different microscopical imaging techniques was applied to examine the changes on the 3D biofilm structure of *P. aeruginosa* which were quantified through performing architectural metrics calculations (substratum area, cell area coverage and biovolume). SeNPs produces an 80% inhibition in the violacein production by *C. violaceum* and a significant effect in *P. aeruginosa* biofilm architecture (a reduction of 80% in the biovolume of the bacterial biofilm was obtained). TeNPs similarly affect violacein production and *P. aeruginosa* biofilm structure but at lower concentration levels. The results obtained suggest an important disruption of the QS signalling system by SeNPs and TeNPs supporting nanotechnology as a promising tool to fight against the emerging problem of bacterial resistance related to bacterial biofilm formation.

Keywords: selenium nanoparticles, tellurium nanoparticles, quorum sensing, antibiofilm activity, biofilm structure.

View Article Online
DOI: 10.1039/C9MT00044E

SIGNIFICANCE TO METALLOMICS

The interaction between nanoparticles with bacterial cells as individual entities has been extensively evaluated. However, in many persistent infections bacteria behave as a cooperative group of bacterial cells coordinated through a Quorum sensing (QS) signalling system that favours, among other factors, the formation of bacteria biofilm. This strategy provides bacteria resistance to host defences or antibiotic treatments. This study presents for first time the effect of SeNPs and TeNPs on different process regulated by QS. Understanding the interaction between nanoparticles and bacterial community behaviour will allow developing new and more efficient strategies for controlling bacterial persistent infections.

1. INTRODUCTION

Several bacterial processes are ruled through a cell-to-cell communication system by means of releasing chemical signal molecules called autoinducers, in a cell density dependent process known as *quorum sensing* (QS). One of the main groups of autoinducers identified as QS signalling molecules in Gram-negative bacteria are the N-acyl-L-homoserine lactones (AHLs). When the microbial population reaches high density, these molecules link to specific receptors promoting the expression of genes related with specific responses such as the production of violacein, antibiotics resistance, biofilm formation and interaction with host.[1-3] Pathogenic bacteria could establish a persistent infection when they adopt a biofilm mode of growth, which results in an increased resistance to antibiotics. Biofilm formation involves the growth of microbial communities attached to a surface and embedded in a self-produced polymeric matrix, providing structural stability along with resistance against traditional antimicrobial agents.[4-6] Disruption of the QS signal is currently explored as an alternative strategy to fight against microbial resistance.[7] In this context, nanotechnology has been considered as a promising approach to tackle persistent bacterial infections. Metal and metal oxide nanoparticles such as silver, copper, zinc oxide and copper oxide nanoparticle are gaining large interest within the scientific community as it is shown in the increasing number of articles in which their potential antimicrobial activity is reported.[8-10] Furthermore, metal/metal oxide nanoparticles are expected not only to inhibit bacterial growth but also to avoid antibiotic resistance mechanism due to their interaction with bacterial cells through different pathways.[9] Likewise, less explored nanoparticles such as metalloids nanostructures have been synthesized at laboratory scale for being used as new antimicrobial nanomaterials with more effectiveness and less toxicity for human cells. For example, selenium nanoparticles (SeNPs) have revealed as interesting tools due to their antioxidant,

anticarcinogenic and antimicrobial properties together with their low toxicity compared with other nanoparticles such as AgNPs and even with other selenium compounds.[11] Tellurium compounds can be found in applications related to solar panels, glasses, rubber, rechargeable batteries, semiconductors and they have been also evaluated for their potential antimicrobial, anti-inflammatory and anticarcinogenic effects therefore, although less investigated, they have been gaining attention for electronics, biotechnology and medical applications.[12,13]

Most of the articles published in the literature on the antimicrobial activity of nanoparticles are focused on their effect in planktonic cultures or in biofilm inhibition.[14-21] However, more studies need to be performed with the aim of understanding how nanoparticles affect bacterial environments in which bacterial QS plays a key role. Evaluating the effect of metal-based nanoparticles in processes regulated by QS along with information on the effect of nanoparticles towards biofilm structure parameters will provide a better knowledge of their effect on bacterial community behaviours that may allow researchers to develop new strategies for controlling biofilm development and consequently to control bacterial resistance.

Hence, in this study the potential of SeNPs and TeNPs of inhibiting different processes regulated by QS (violacein production and biofilm development) was evaluated with the aim of giving a deeper insight into the influence of these nanoparticles on bacterial communication. The inhibition of violacein production of *C. violaceum* by these nanoparticles was assessed by using two different strains, being one of them an AHL-deficient mutant. Furthermore, the antibiofilm potential of SeNPs and TeNPs was also proved against a strain of *P. aeruginosa*, paying special attention to the changes induced by these nanoparticles in the structure of the biofilm. For this purpose, data from the crystal violet staining assay were combined with the information provided by a panel of

imaging techniques including traditional microscopy techniques such as electron (TEM) and optical microscopy (DICM and PCM), and advanced imaging techniques such as confocal laser scanning microscopy (CLSM) together with digital image processing.

2. METHODS

2.1 Synthesis, purification and characterization of selenium nanoparticles and tellurium nanoparticles

SeNPs were synthesized following the procedure described by Palomo *et al.* (2017).[22] The method is based on the chemical reduction of sodium selenite with ascorbic acid in presence of hydroxyethyl cellulose (HEC) as coating agent. In case of TeNPs, a similar procedure was applied but the chemical reduction of tellurium salt (K_2TeO_3) was performed with gallic acid and, similarly, HEC was employed as coating agent. The resulting SeNPs and TeNPs were purified through a dialysis process and characterized in terms of size and composition by TEM (JEOL JEM 2100; USA) equipped with an Energy-Dispersive X-ray Spectroscopy (EDXS) microanalysis composition system (Oxford Inca). More than 1500 SeNPs and TeNPs dispersed in about 20 TEM photos were viewed to measure the size distribution either in water or in LB media

2.2. Bacterial strains culture

Two *C. violaceum* strains were used: *C. violaceum* ATCC 12472 and the AHL-deficient mutant CV026. Both strains were aerobically cultured in 15 mL Falcon® with LB media at 30ºC during 14-18 h under stirring conditions (120 rpm). Optical density (OD) of bacterial cultures was adjusted to 0.2 at 620 nm before performing the QS inhibition experiments. Likewise, *P. aeruginosa* cultures (Department of Genetics, Physiology and Microbiology culture collection) were grown and the resulting bacterial suspensions

were diluted with LB to reach an optical density (OD) value of 0.1 at 620 nm before performing biofilm assays.

2.3 Violacein production assays

The *C. violaceum* ATCC 12472 strain produces the pigment violacein in a QS mediated process induced by N-acyl homoserine lactones (AHLs) while CV026 strain is deficient in the autoinducer synthase requiring the exogenous addition of AHL to produce violacein. Both strains are usually employed for evaluating the QS inhibition of different substances.[23-26]

Both strains of *C. violaceum* (0.2 OD at λ_{620nm}) were cultivated simultaneously in presence of 0, 10, 100 and 250 mg Se L^{-1} in sterile Eppendorf tubes. For the experiments carried out with TeNPs, lower concentrations were added to bacterial cultures (10, 50, 100 and 250 µg Te L^{-1}) as they exhibit higher toxicity against *C. violaceum*. Tubes were subsequently incubated at 30ºC under shaking at 120 rpm during 24 h. Eight replicates were performed for each concentration. The same protocol was applied when using the strain CV026 although, in order to induce the violacein production, the autoinducer N-hexanoyl-L-homoserine lactone (C6-HSL) (Sigma-Aldrich) (10 mM) was previously added to the culture media.

After 24 h incubation, tubes were centrifuged at 13000 rpm for 15 min to allow the insoluble violacein settle down. Afterwards, 1 ml of DMSO was added to the resulting pellet. The mixture was vortexed until the violacein was completely solubilized and centrifuged at 13000 rpm during 10 min. 250 µL of supernatant containing the solubilized violacein were placed in a 96 flat-bottom well microtiter plate. The absorbance was measured with a microplate reader at a wavelength of 570 nm.

To check whether changes in violacein production were related to modifications in QS processes or were due to a decrease in cell viability produced by the antibacterial activity of SeNPs, strains of ATCC 12472 and CV026 were incubated with different concentrations of SeNPs (0, 10, 100 and 250 mg Se L^{-1}) and TeNPs (0, 10, 50, 100 and 250 µg L^{-1}) during 24h. After that, an aliquot of each culture was serially diluted and 100 µL were spread on LB-agar plates. The plates were incubated at 30ºC for 48 h and the grown bacterial CFU (Colony Forming Units) were counted.

2.4 Biofilm development in presence of SeNPs and TeNPs. Crystal violet assays

The effect of SeNPs and TeNPs on *P. aeruginosa* biofilm formation was evaluated at different nanoparticle concentrations: 10, 100 and 250 mg Se L^{-1} and 0.1, 0.5, 1, 5, 25, 50 and 75 mg Te L^{-1}. The experiments were conducted following the procedure described by Merritt *et al*. (2011). [27] 25 µL of SeNPs or TeNPs dispersions were placed into a well of a sterile polystyrene non-treated 96 flat-bottom well microtiter plate (Costar) before adding 75 µL of the diluted *P. aeruginosa* culture (0.1 OD_{620}). Then the plates were incubated at 28ºC under stirring (120 rpm) during 24 h. Eight replicates of each experiment were done and a negative (LB medium) and a positive control (diluted bacterial culture without adding selenium or tellurium) were performed in parallel. Afterwards, non-adherent bacterial cell suspensions were discarded. The biofilm adhered to the wells was subsequently stained with 125 µL of 0.1 % (w/v) crystal violet solution and kept in darkness during 15 min. The excess of dye in the plates was removed with Milli Q-water. Finally, 200 µl of glacial acetic acid 30% (w/v) were added to each stained well to dissolve the stain adsorbed to the bacterial biofilm. The absorbance was then measured at 570 nm at room temperature by using a Varioskan LUX Multimode Microplate Reader (Thermo-Fisher). The average of the results was compared with those obtained from the positive controls.

The capability of SeNPs and TeNPs for removing biofilms once formed was assessed according to the procedure previously described with a slight modification. In this case, biofilms were first developed and,SeNPs or TeNPs were subsequently added.

2.5 Microscopic analysis of bacterial biofilms

The effect of SeNPs and TeNPs on *P. aeruginosa* biofilm architecture was evaluated by Confocal Laser Scanning Microscopy (CLSM, Leica SP2 with Leica DFC 350 FX digital camera). For this purpose, biofilms were grown in flat bottom sterile non-treated 24-well plates (Thermo Fisher Scientific) in presence of SeNPs at 10, 100 and 250 mg Se L^{-1} and TeNPs at 1, 25 and 125 mg Te L^{-1}. Once the incubation period was completed, the supernatant with non-adherent cells were carefully removed and the biofilm was stained with SYTO 9 and PI fluorescent dyes. After 15 min incubation, between four and six CLSM image stacks of each plate were acquired from random positions using a 20× lens leading to a total area under investigation of 7.76-11.64 × 10^5 μm^2. Images were collected at 2 μm intervals from the bottom of the surface of the plate to the top of the biofilm, and the number of images in each stack varied according to the thickness of the biofilm. All the images were collected with a resolution of 1,024 × 1,024 pixels. Images stacks were evaluated by using the Image J and bioImage L v.2.1 software packages.[28]

Additional information on the structural changes of biofilm by nanoparticles was obtained by applying Differential Interference Contrast (DICM, Nikon Eclipse 80i with a Nikon Digital Sight DS-Fi1 camera) and Phase Contrast (PCM, Olympus BX50 with a Canon Power Shot A620 digital camera) microscopy.

View Article Online
DOI: 10.1039/C9MT00044E

2.6 Statistical analysis

The results obtained from the experiments were expressed as the mean ± standard deviation (SD). Statistically significant differences between groups were detected by a two-way analysis of variance (ANOVA) and by using Statgraphics v6.0 software (Manugistics, Rockville, USA). Only results with a p-value of less than 0.05 were considered to be statistically significant different.

3. RESULTS AND DISCUSSION

3.1 Effect of Luria-Bertani culture medium in nanoparticles stability

SeNPs and TeNPs were successfully synthesized through the procedure described in section 2.1. TEM micrographs evidenced the presence of spherical and dispersed SeNPs and TeNPs with an average diameter size of 90±10 and 125±40 nm respectively. Furthermore, EDXS analysis confirmed the presence of Se ((L_α (1.4 keV), K_α (11.22 keV) and K_β (12.49 keV)) and Te (L_α (3.77keV), K_α (27.47 keV) and K_β (31.72 keV)), in both cases (Figure 1a and 1c). Additionally, the electron diffraction pattern confirmed the non-microcrystalline structure of both types of nanoparticles. The nanoparticles were also characterized in LB with the aim of assessing their stability in presence of the culture medium used for growing the bacteria: 85±15 nm and 130±35 nm were the average diameter size for SeNPs and TeNPs respectively. No significant differences between average size diameter and morphology of SeNPs and TeNPs dispersed in the synthesis media (Figure 1a and 1c) and in LBS media (Figure 1b and 1d) were detected.

3.2 Effect of SeNPs and TeNPs on *C. violaceum* quorum sensing regulated violacein production

During last years, disruption of the QS signal has been explored as new strategy for antimicrobial therapy with the aim of opening new alternatives to fight against microbial resistance. Briefly, the repression of cell-to-cell communication may take place at three different levels: (i) by inhibiting the synthesis of signal molecules, (ii) by limiting the accumulation, exchange and transport of QS signal and (iii) by disturbing signal perception and response (Figure 2a).[29] Most of the reported studies on the effect of nanoparticles on QS processes have been focused on quantifying the modification of QS signal instead of evaluating at what stage cell-to-cell communication is disturbed. In this sense, *C. violaceum* has been widely employed as a model organism in QS research due to its capacity of producing the purple pigment violacein through a QS regulated process.[23-26] In the current study, a simple procedure was applied to evaluate at which stage nanoparticles alter the QS process. For instance, a decrease in violacein production by the strain ATCC 12472 accompanied with no variation in violacein production by the CV026 mutant strain suggests a disruption of the biosynthesis production of the autoinducer (Figure 2a step i). In contrast, a decrease in violacein production by CV026 in presence of AHL indicates that the recognition of the QS signal and reception might be interfered as long as the production of the purple pigment in the strain ATCC 12472 is not decreased. To understand the last statement, it is important to keep in mind that CV026 cannot produce the QS signal responsible of the violacein production (Figure 2a step ii and iii).

Figure 2b evidences an 80% decrease in violacein production by ATCC 12472 strain in presence of 250 mg Se L^{-1} while the pigment production was kept constant by CV026 strain where the exogenous addition of C6-HSL is not needed as this strain is able to

intrinsically produced violacein as stated in Methods (section 2.3). Moreover, it was proved that the viability of both strains remains unaffected during experimental with SeNPs (Figure 2c and 2d). Therefore, changes on violacein production seem not to be a consequence of cell population density reduction and may be related to the interruption of bacterial QS. Consequently, in agreement with our previous statement, SeNPs might affect in a greater extent the biosynthesis of the autoinducer (Figure 2a step i) rather than to disturb signal perception and response (Figure 2b step ii and iii).

Regarding to TeNPs, 50 µg Te L^{-1} of TeNPs was enough to inhibit the 70% of the violacein production by CV026 while the pigment production was kept constant by ATCC 12472 strain. However, a higher concentration of TeNPs caused the inhibition of the 80% of the violacein production in both, CV026 and ATCC 12472 (Figure 3a). As for SeNPs, viability of both strains remains unaltered during the experiment (Figure 3c and 3c). According to the aforementioned comments, the presence of TeNPs as a concentration level of 50 µg Te L^{-1} mainly affect processes related to the signal perception and response rather than those linked with the synthesis of the autoinducer. Nevertheless, when higher levels of TeNPs were supplemented to the bacterial culture it was not possible to determine which of QS steps were disturbed in a greater extent since both strains were similarly altered.

It is worth mentioning that the presence of nanoparticle of different composition leads to different responses in QS system. SeNPs might affect in a greater extent the biosynthesis production of the autoinducer whereas TeNPs seem to disturb the signal perception and response. Moreover, differences in the quantity of nanoparticles that is needed to reach one of the responses were also observed. No changes in violacein production of CV026 were achieved in presence of 250 mg Se L^{-1} of SeNPs while only 50 µg Te L^{-1} of TeNPs were needed for decreasing the violacein production in this

strain. Moreover, the violacein production by ATCC 12472 was modified in presence of 250 mg Se/L while only 100 µg Te L^{-1} of TeNPs were required to reach the same effect.

3.3 Antibiofilm activity of SeNPs and TeNPs assessed by the colorimetric method

Another process regulated by QS is the formation of biofilms which represents a key step in the pathogenicity of many bacterial species. In the current study, the antibiofilm activity of SeNPs and TeNPs on *P. aeruginosa* was assessed by using the colorimetric method described in section 2.4. Figure 4a evidenced that the production of biofilm by *P. aeruginosa* was significantly inhibited in presence of 100 mg Se/L as SeNPs (Figure 3a) suggesting a reduction of the 60% of the biofilm developed by the bacteria. Furthermore, the presence of 250 mg Se L^{-1} SeNPs exhibits an increased ability to inhibit biofilm formation in more than the 70%. No changes on *P. aeruginosa* viability were observed when cultures were exposed to the assayed NPs concentrations (data not shown); therefore changes in developed biofilms were not due to a reduction of bacterial population density. However, when the biofilm was previously formed (Figure 4b), only a 15% of biofilm reduction in presence of 250 mg Se L^{-1} was achieved. Therefore, from the results obtained for both experiments it can be highlighted that SeNPs showed more effectiveness in inhibiting the biofilm development rather than in removing the biofilms once formed. This fact agrees with our previous results, in which SeNPs showed the ability of interrupting bacterial QS at certain step (disruption of the biosynthesis production of the autoinducer) and thus to interfere with biofilm formation. On the other side, when biofilm is already formed, the QS signalling is a less critical stage and SeNPs are less effective in removing pre-established biofilms.

With reference to experiments carried out with TeNPs, it was evidenced an 80% of biofilm reduction at concentration levels higher than 25 mg Te L^{-1} (Figure 4c). Once

again, the population density of *P. aeruginosa* was no affected by the NPs concentrations employed (data not shown). In contrast to SeNPs, Figure 4d showed that 0.1-5 mg Te L^{-1} concentration of TeNPs was able to reduce just the 30% of biofilm once formed. In this particular case, it was difficult to establish a correlation between *C. violaceum* and *P. aeruginosa* data since at concentration levels higher than 5 mg L-1, it was not possible to determine which the QS step was disturbed in a greater extent, since, as it is was previously mentioned, both strains (ATCC 12472 and CV026) were similarly altered.

However, it is to point out the presence of a black colour in those wells where TeNPs were supplemented with more than 5 mg Te L^{-1} and after 24h of culture incubation in biofilm removing experiments. This fact lead to erroneous absorbance readings when performing colorimetric experimental revealing non-accurate results which might explain the increase of percentage of biofilm formation observed at concentration higher than 5 mg Te L^{-1} (Figure 4d). Changes in the colour of growing biofilm from nearly colourless to deep black can be explained by the presence of biogenic tellurium nanostructures. Figure 4e showed how *P. aeruginosa* was able to modify the shape of tellurium nanoparticles from spherical to nanorods structures being the latter responsible of the black colour of the solution. This fact, the transformation of metal and metalloids ions into extracellular nanomaterials by bacterial cells (and also biofilms), has been previously reported as a mechanism to reduce toxicity.[13] However, as far as we know, this particular morphological transformation from spherical TeNPs to nanorods after being exposed to *P. aeruginosa* biofilm has not been reported to date. Sinha *et al.* (2014) and Gates *et al.* (2002) described a similar process by which selenium nanorods can be formed from selenium nanospheres as an aggregation and dissolution process.[30,31] So, a similar mechanism could likely occur when spherical

TeNPs are in contact with *P. aeruginosa* biofilm, and this transformation can be explained by the less toxicity of nanorods structures. The fact that the black colour only appeared when bacterial biofilm was present suggest bacterial biofilm as responsible of the nanospheres transformation into nanorods instead of planktonic bacterial cells.

3.4 Effect of SeNPs and TeNPS on biofilm architecture evaluated by different imaging approaches

Previous results have demonstrated that SeNPs and TeNPs disturb biofilm production. The Cristal violet colorimetric assay enables the quantification of developed biofilms but it does not allow examining the structural properties of the biofilm, which is needed for properly evaluating changes induced in the architecture and cell distribution in the biofilm. Therefore, the impact of nanoparticles on *P. aeruginosa* mature biofilm was evaluated by different imaging techniques: CLSM, DICM and PCM. Figure 5(a) and (b) show 3D projections and CLSM micrographs respectively of *P. aeruginosa* biofilm structure, with or without SeNPs and after 24h of incubation time. CLSM imaging clearly revealed a highly heterogeneous structure of the biofilm in absence of SeNPs rendering to a low substratum coverage percentage (Table 1). From the obtained images, bacterial cells seemed to be accumulated around the network structure of the extracellular polymerics substances (EPS) produced by the bacteria. However, the presence of SeNPs notably altered the microbial biofilm structure with respect to the control. As it is shown, in presence of SeNPs, *P. aeruginosa* developed a heterogeneous structure containing discrete separate micro-aggregates. These significant changes in the 3D biofilm architecture led up to a 98% reduction in biovolume (the overall volume of cells in the observation field) as SeNPs concentration increases (Table 1). Despite the striking reduction in biovolume, the percentage of viable cell in the biofilm remained constant or slightly decreased with increasing SeNPs concentration (Table 1). This fact

was corroborated by performing a viability analysis in the biofilm treated with SeNPs using fluorescent dyes (data not shown). In parallel to the reduction of the biovolume, the cell area coverage (and therefore the percentage of cells) suffered also a great diminution which evidenced less effectiveness in the surface colonization and distortion in the biofilm architecture (Table 1).

The images provided by PC and DIC microscopy (Figure 4c and Figure 4d) showed a heterogeneous biofilm structure similar to that previously detected by CLSM. Bacterial biofilm seems to be continuous and heterogeneous in the untreated glass slide. In contrast, the presence of SeNPs resulted in a significant structural distortion of the biofilm architecture where nanoparticles seemed to be attached to the biofilm surface as revealed by the distinctive red colour of SeNPs.

Similar images were acquired form *P. aeruginosa* biofilm treated with different concentration of TeNPs (1, 25 and 125 mg Te L^{-1}). Once again, CLSM micrographs (Figure 6a and 6B) showed highly heterogeneous biofilm with bacterial cells attached around the network structure of the EPS at the lowest concentration of TeNPs. However, the microbial structure of *P. aeruginosa* biofilm was visible altered when the concentration of TeNPs increased forming heterogeneous structure containing separate microaggregates. These changes in 3D biofilm structure were accompanied by a biovolume reduction up to the 97% at 125 mg Te L^{-1} (Table 2). While in the case of SeNPs the percentage of viable cells remained constant, the presence of TeNPs produced losses in cell viability (Table 2). The reduction in the biovolume was also accompanied by a reduction in the cell area coverage. Phase contrast and DIC images obtained from experiments carried out with TeNPs were not included in the manuscript The white colour of TeNPs makes difficult to determine their location of the nanoparticles as it was the case for the red SeNPs (Figures 5c and 5d).

Regarding to the results related to both nanoparticles, it is worth highlighting that the application of imaging techniques allowed us to directly observe SeNPs and TeNPs activity within the bacterial biofilm structure and hypothesize about the mechanism of the antimicrobial effect of SeNPs. The proposed path may consist in three consecutive steps: transport of NPs to the confines of the biofilm, attachment to the surface and finally migration within the biofilm. These results are in agreement with the experimental observation made by other authors when using other type of nanoparticles.[32]

Finally, it is worth mentioning that different values in biofilm inhibition were provided by CLSM and colorimetric methods. Differences can be attributed to the different information provided by both techniques. Crystal violet assay allows quantifying biofilm biomass through the staining of the whole microbial population as well as other components present in the biofilm matrix. Although is one of the most common methods for evaluating microbial biofilms, it presents some drawbacks mainly associated to the washing step employed for removing unattached cells that may lead to a poor reproducibility of the results and erroneous conclusions. CLSM allows obtaining three-dimensional examination of the biofilm and information on structural parameters such as biofilm biovolume as well as spatial distribution of viable and non-viable bacteria within the confines of a biofilm. [33] Otherwise, when nanoparticles are involved in crystal violet assays, erroneous results could be obtained. Thuptimdang *et al.* (2017) reported differences in biomass results from crystal violet staining experiments and CLSM measurements when AgNPs were tested as antibiofilm agent. Variations in results were attributed to the ability of the dye to stain all biofilms components including EPS and live and dead cells whereas the physical characteristics calculated by imaging software programs are exclusively based on 3D images of cell populations.[34]

Additionally, nanoparticles can interact with either the EPS of the biofilm matrix or with the microplate surface producing a non-specific staining which may contribute to inaccurate conclusions.

4. CONCLUSIONS

Results presented in this work suggest that metalloid nanoparticles such as SeNPs and TeNPs disturb QS signalling system and hence bacteria-bacteria communication. It has been showed that these nanoparticles produce the inhibition of QS-mediated violacein synthesis in *C. violaceum* and biofilm formation in *P. aeruginosa*. SeNPs greatly affect the violacein production (80%) in *C. violaceum* strain ATCC 12472 suggesting the interruption of QS signal biosynthesis by nanoparticles whereas TeNPs might mostly affect processes related to the signal perception and response. So, nanoparticles seem to disturb QS processes depending on their characteristics. Furthermore, results from colorimetric assays showed that SeNPs nanoparticles are more effective when inhibiting biofilm formation than removing the pre-established biofilm, which is in agreement with ability of SeNPs to interrupt the bacterial signalling needed for developing biofilm. In case of TeNPs, lower concentration was required to cause a similar inhibition values in *P. aeruginosa* biofilm. Finally, a multiplatform of imaging techniques along with bioinformatics tools have allowed the evaluation of the mechanism by which SeNPs and TeNPs could behave as antibiofilm agents. Digital image processing of CLSM and microscopy techniques have shown that both nanoparticles produce a severe distortion in the biofilm structure developed by *P. aeruginosa*. The alteration of the organized structure of biofilm may influence biofilm antibiotic tolerance, thus reducing antibiotic resistance. Data from performing architectural metric calculations evidenced that decreases of biofilm structure stability is associated with a biovolumen reduction.

The present study provides for first time information on the mechanisms by which metalloid nanoparticles disturb bacterial QS communication and population behaviour. The results obtained open new approaches to fight against bacterial persistent infections, multidrug resistance or any other QS-related process of medical, biotechnological or environmental concern.

ACKNOWLEDGEMENTS

The authors thank the Spanish Commission of Science and Technology (CTQ2017-83569-C2-1-R and CTM2016-76491-P) and the Comunidad of Madrid and European funding from FSE and FEDER programs (project S2018/BAA-4393, AVANSECAL-II-CM). We also thank the Cytometry and Fluorescence Microscopy Centre (Complutense University of Madrid) for technical assistance.

REFERENCES

1. T. Defoirt, Quorum-Sensing systems as targets for antivirulence therapy, *Trends Microbiol.*, 2018, **26(4)**, 313-328.

2. M. Whiteley, S.P. Diggle, E.P. Greenberg, Bacterial quorum sensing: the progress and promise of an emerging research area, *Nature*, 2017, **551(7680)**, 313-320.

3. N.B. Turan, D.S. Chormey, C. Buyukpinar, G.O. Engin, S. Bakirdere, Quorum sensing: Little talks for an effective bacterial coordination, *Trends Anal. Chem.*, 2017, **91**, 1-11.

4. T.R.Garrett, M. Bhakoo, Z. Zhang, Bacterial adhesion and biofilms on surfaces, *Prog. Nat. Sci.*, 2008, **18**, 1049–1056.

5. A. Kumar, A. Alam, M. Rani, N.Z. Ehtesham, S.E. Hasnain, Biofilms: survival and defence strategy for pathogens, *Int. J. Med. Microbio.*, 2017, **307(8)**, 481-489.

6. N. Hoiby, O. Ciofu, H.K. Johansen, Z. Song, C. Moser, P.O. Jensen, S. Molin, M. Givskov, T. Tolker-Nielsen, T. Bjarnsholt, The clinical impact of bacterial biofilms, *Int. J. Oral Sci.,* 2011, **3**, 55–65.

7. V.C. Kalia, S.K.S. Patel, C. Kang, J.K. Lee, Quorum sensing inhibitors as antipathogens: biotechnological applications, *Biotechnol. Adv.*, 2019, **37(1)**, 68-90.

8. A. Raghunath, E. Perumal, Metal oxide nanoparticles as antimicrobial agents: a promise for the future, *Int. J. Antimicrob. Agents*, 2017, **49(29)**, 137-152.

9. Y.N. Slavin, J. Asnis, U.O. Häfeli, H. Bach, Metal nanoparticles: understanding the mechanisms behind antibacterial activity, *J. Nanobiotechnology*, 2017, **15**, 1-65.

10. L. Wang, C. Hu, L. Shao, The antimicrobial activity of nanoparticles: Present situation and prospects for the future*, Int. J. Nanomedicine*, 2017,**12**, 1227-1249.

11. S. Chhabria, K. Desai, Selenium nanoparticles and their applications. In book Encyclopedia of Nanoscience and Nanotehnology, 2016, Publisher: American Scientific Publishers, Editors: Dr H. Nalwa, pp.1-32.

12. L.A. Ba, M. Döring, V. Jamier, C. Jacob, Tellurium: and element with great biological potency and potential. *Org. Biomol. Chem.*, 2010, **8**, 4203-4216.

13. R.J. Turner, R. Borghese, D. Zannoni, Microbial processing of tellurium as a tool in biotechnology. *Biotechnol. Adv.*, 2012, **30**, 954-963.

14. M. Stozoff, S.Q. Wang, J. Webster, Efficacy and mechanism of selenium nanoparticles as antibacterial agents, *Front. Bioeng. Biotechnol.*, 2016, Conference Abstract: 10th World of Biomaterial Congress.

15. G. Khiralla, B. El-Deeb, Antimicrobial and antibiofilm effects of selenium nanoparticles on some foodborne pathogens, *LWT Food Sci.Technol,* 2014, **63(2)**,1001-1007

16. M. Shakibaie, H. Forootanfar, Y. Golkari, T. Mohammadi-Khorsand, M. J. Shakibaie, Anti-biofilm activity of biogenic selenium nanoparticles and selenium dioxide against clinical isolates of *Staphylococcus aureus, Pseudomonas aeruginosa*, and *Proteus mirabilis, J. Trace Elem. Med. Biol.*, 2015, **29**, 235-241.

17. X. Huang, X. Chen, Q. Chen, Q. Yu, D. Sun, J. Liu, Investigation of functional selenium nanoparticles as potent antimicrobial agents against superbugs., *Acta Biomater.*, 2016, **30**, 397-407.

18. E. Cremonini, M. Boaretti, I. Vandecandelaere, E. Zonaro, T. Coenye, M. LLeo, S. Lampis, G. Vallini, Biogenic selenium nanoparticles synthesized by *Stenotrophomonas maltophilia* SeITE02 loose antibacterial and antibiofilm efficacy as a result of the

progressive alteration of their organic coating layer. *Microb. Biotechnol.,* 2018, **11**, 1037-1047.

19. B. Zare, M.A. Faramarzi, Z. Sepehrizadeh, M. Shakibaie, S. Rezaie, A.R. Shahverdi, Biosynthesis and recovery of rod shaped tellurium nanoparticles and their bactericidal activities, *Mater. Res. Bull.,*2012, **47**, 3719-3725.

20. E. Zonaro, S. Lampis, R.J. Turner, S.J.S Qazi, G. Vallini, Biogenic selenium and tellurium nanoparticles synthesized by environmental microbial isolates efficaciously inhibit bacterial planktonic cultures and biofilms, Front. Microbiol., *2015*, **6**, 584.

21. D.C. Vaigankar, S.K. Dubey, S.Y. Mujawar, A. Costa, S.K. Shyama, Tellurite biotransformation and tetoxification by *Shewanella baltica* with simultaneous synthesis of tellurium nanorods exhibiting photo-catalytic and anti-biofilm activity, *Ecotox. Environ. Safety*, *2018*, **165**, 516-526.

22. M. Palomo-Siguero, Y. Madrid. Exploring the behavior and metabolic transformations of SeNPs in exposed lactic acid bacteria. Effect of nanoparticles coating agent. *Int. J. Mol. Sci.*, 2017,**18 (8),**1712 .

23. M.S. Wagh, R.H. Patil, D.K. Thombre, M.V. Kulkarni, W.N. Gade, B.B. Kale, Evaluation of anti-quorum sensing activity of silver nanowires. *Appl. Microbiol. Biotechnol.*, 2013, **97**, 3593-3601.

24. K. Naik, M. Kowshik. Anti-quorum sensing activity of AgCl-TiO_2 nanoparticles with potential use as active food packaging material, *J. Appl. Microb.*, 2014, **117 (4)**, 972-983.

25. B.R. Singh, B.N Singh, A. Singh, W. Khan, A. Naqvi, H.B. Singh, Mycofabricated biosilver nanoparticles interrupt *Pseudomonas aeruginosa* quorum sensing sytems, *Sci. Rep.,* 2015, **5**,13719.

26. N.A. Al-Shabib, F.M. Husain, F. Ahmed, R.A. Khan, I. Ahmad, E. Alsharaeh, M.S. Khan, A. Hussain, M.T. Rehman, M. Yusuf, I. Hassan, J.M. Khan, G.M. Ashraf, A. Alsalme, M.F. Al-Ajmi, V.V. Tarasov, G. Aliev, Biogenic synthesis of zinc oxide nanostructures from *Nigella sativa* seed: Prospective role as food packaging material inhibiting broad-spectrum quorum sensing and biofilm, *Sci. Rep.,* 2016, **6**, 36761.

27. J.H. Merritt, D.E. Kadouri, G.A. O'Toole, Growing and analyzing static biofilms, *Curr. Protoc.Microb.,* 2011, **1**, 1–18.

28. L.E. Chavez de Paz, Image analysis software based on color segmentation for characterization of viability and physiological activity of biofilms, *J. App. Environ. Microbiol.*, 2009, **75,** 1734–1739.

29. C. Grandclement, M. Tannieres, S. Morera, Y. Dessaux, D. Faure. Quorum quenching: role in nature and applied developments. *FEMS Microb. Rev.*, 2016, **40**, 86-116.

30. A.K. Sinha, A.K. Sasmal, S.K. Mehetor, M. Pradhan, T. Pal, Evolution of amorphous selenium nanoballs in silicone oil and their solvent induced morphological transformation. *Chem. Commun.*, 2014, **50**, 15733-15736.

31. B. Gates, B. Mayers, B. Cattle, Y. Xia, Synthesis and characterization of uniform nanowires of trigonal selenium, *Adv. Funct. Mater.,* 2002, **12 (3)**, 219-227.

32. K. Ikuma, A.W. Decho, B.L.T Lau, When nanoparticles meet biofilms –Interactions guiding the environmental fate and accumulation of nanoparticles, *Front. Microbiol.,* 2015, **6**, 1–6.

33. J. Azeredo, N.F. Azevedo, R. Briandet, N. Cerca, T. Coenye, A.R. Costa, M. Desvaux, G. Di Bonaventura, M. Hébraud, Z. Jaglic, M. Kačániová, S. Knøchel, A.Lourenço, F. Mergulhão, R.L. Meyer, G. Nychas, M. Simões, O. Tresse, C. Sternberg, Critical review on biofilm methods, *Crit. Rev. Microbiol*., 2017, **43,** 313–351.

34. P. Thuptimdang, T. Limpiyakorn, E. Khan, Dependence of toxicity of silver nanoparticles on *Pseudomonas putida* biofilm structure. *Chemosphere*, 2017, **188**,199–207.

Figure captions

Figure 1. Transmission electron microscopy (TEM) images and X-ray energy dispersive spectroscopy (EDXS) spectrum of SeNPs and TeNPs dispersed in (a,c) synthesis and (b,d) LB media.

Figure 2. (a) QS-signal pathways that can be affected by nanoparticles (adapted from Grandclement *et al.* (2015).[29] (b) Evaluation of violacein production by *C.violaceum* (ATCC 12472 and CV026) in presence of different concentrations of SeNPs. Bacterial CFU counted from the viability test of *C. violaceum* CV026 (c) and *C. violaceum* ATCC 12472 (d). Columns with asterisks (*) indicate statistically significant differences ($p < 0.05$) between the control and the tested concentrations.

Figure 3. (a) Evaluation of violacein production by *Chromobacterium violaceum* (ATCC 12472 and CV026) in presence of different concentrations of TeNPs. Bacterial CFU counted from the viability test of *C. violaceum* CV026 (b) and *C. violaceum* ATCC 12472 (c). Columns with asterisks (*) indicate statistically significant differences ($p < 0.05$) between the control and the tested concentrations.

Figure 4. Percentage of biofilm formation related to the inhibition assay with *P. aeruginosa* (a,c) and biofilm removing ability (b,d) in presence of increasing concentrations of SeNPs and TeNPs respectively. e) Biogenic tellurium nanorods observed when concentrations over 5 mg Te L^{-1} of TeNPs were employed. Data are expressed as the mean±SD (n=8). Wells where biofilm was produced in absence of SeNPs or TeNPs were labelled as the cero point of concentration and designed as control. Columns with asterisks (*) indicate statistically significant differences ($p < 0.05$) between the control and the tested concentrations.

View Article Online
DOI: 10.1039/C9MT00044E

Figure 5. (a) 3D distribution of the analysed biofilm population obtained from one of the confocal z-stacks using bioImageL software, (b) examples of different CLSM images composing a stack (different sections of a biofilm population). Bacteria with intact cell membranes are stained fluorescent green whereas bacteria with damaged membranes are stained fluorescent red; (c) phase contrast-microscopy microphotographs and (d) differential interference contrast microscopy images. All of them correspond to *P. aeruginosa* biofilm developed in presence of different concentrations of SeNPs after 24 h of exposure.

Figure 6. (a) 3D distribution of the analysed biofilm population obtained from one of the confocal z-stacks using bioImageL software and (b) examples of CLSM images composing a stack (different sections of a biofilm population). Bacteria with intact cell membranes are stained fluorescent green whereas bacteria with damaged membranes are stained fluorescent red. All of them correspond to *P. aeruginosa* biofilm developed in presence of different concentrations of TeNPs after 24 h of exposure.

View Article Online
DOI: 10.1039/C9MT00044E

Table 1. Analysis of biofilms developed by *P. aeruginosa* in presence and absence of SeNPs. Data were calculated from the images obtained by CLSM with bioImage_L software.

SeNPs (mgSe L^{-1})	Substratum area (μm^2)	Cell area coverage (μm^2)	Coverage (%)	Biovolume (μm^3)	Biovolume reduction (%)	Viable cells biovolume (%)
0	775809	34886	4	294487	----	95
10	775809	21055	3	80864	70	90
100	775809	17372	2	68716	80	100
250	775809	10490	1	6937	98	99

View Article Online
DOI: 10.1039/C9MT00044E

Table 2. Analysis of biofilms formed by *P. aeruginosa* in presence and absence of TeNPs. Data were calculated from the images obtained by CLSM with bioImage_L software.

TeNPs (mgTe L^{-1})	Substratum area (um^2)	Cell area Coverage (um^2)	Coverage (%)	Biovolume (um^3)	Biovolume reduction (%)	Viable cells biovolume %
0	973640	34345	4	148361	----	83
1	973640	35345	4	123177	17	85
25	973640	33894	4	112533	30	70
125	973640	2887	1	3619	97	79

Figure 1.

View Article Online
DOI: 10.1039/C9MT00044E

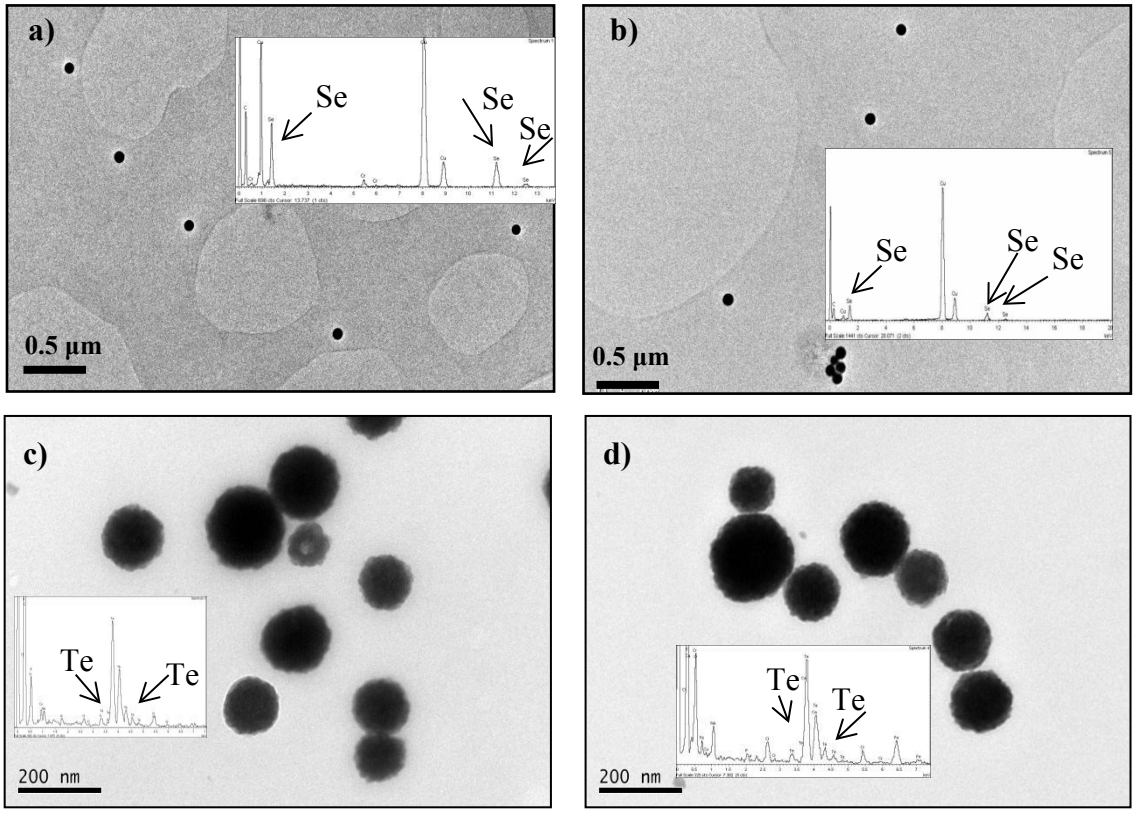

View Article Online
DOI: 10.1039/C9MT00044E

Figure 2

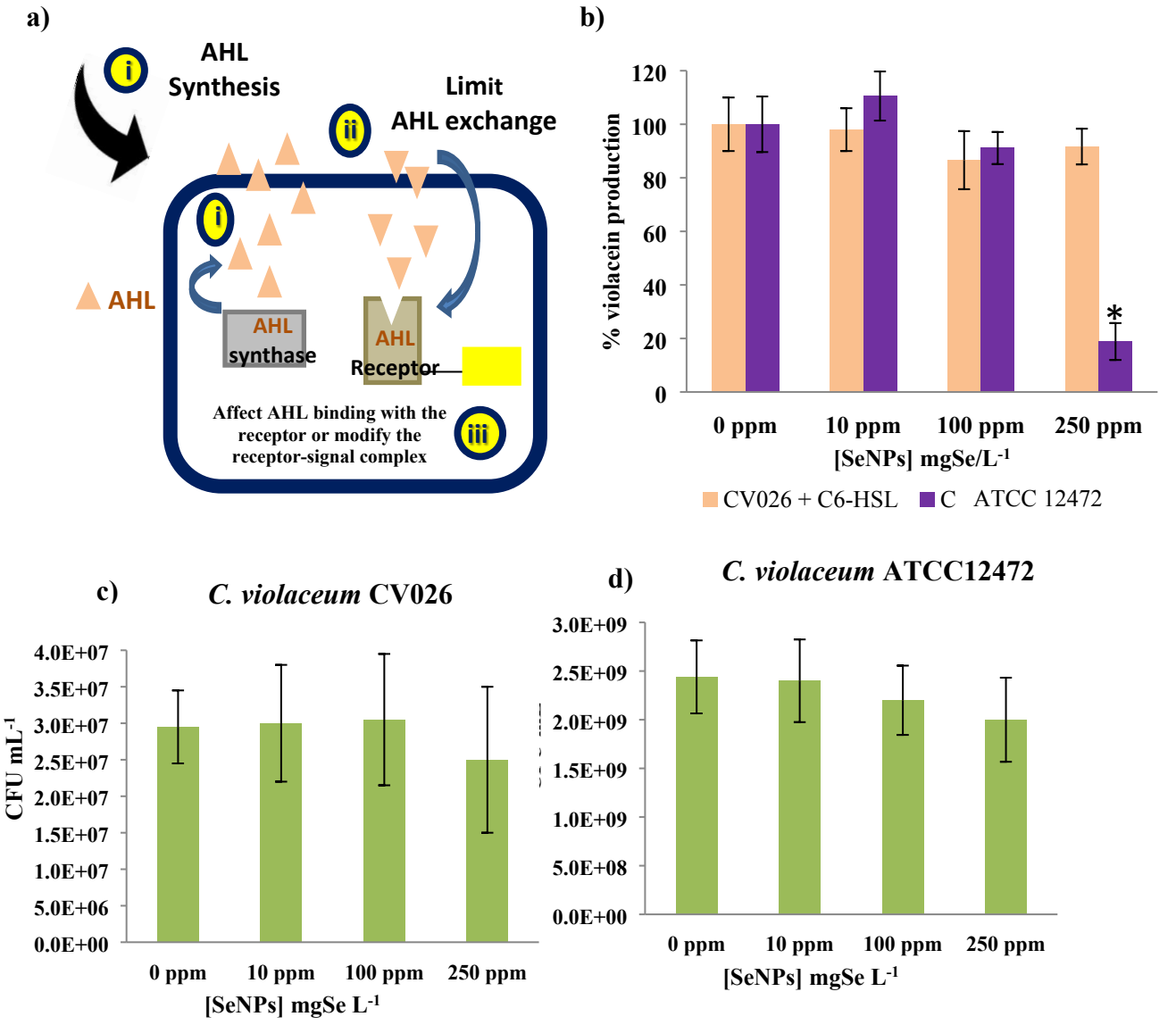

View Article Online
DOI: 10.1039/C9MT00044E

Figure 3

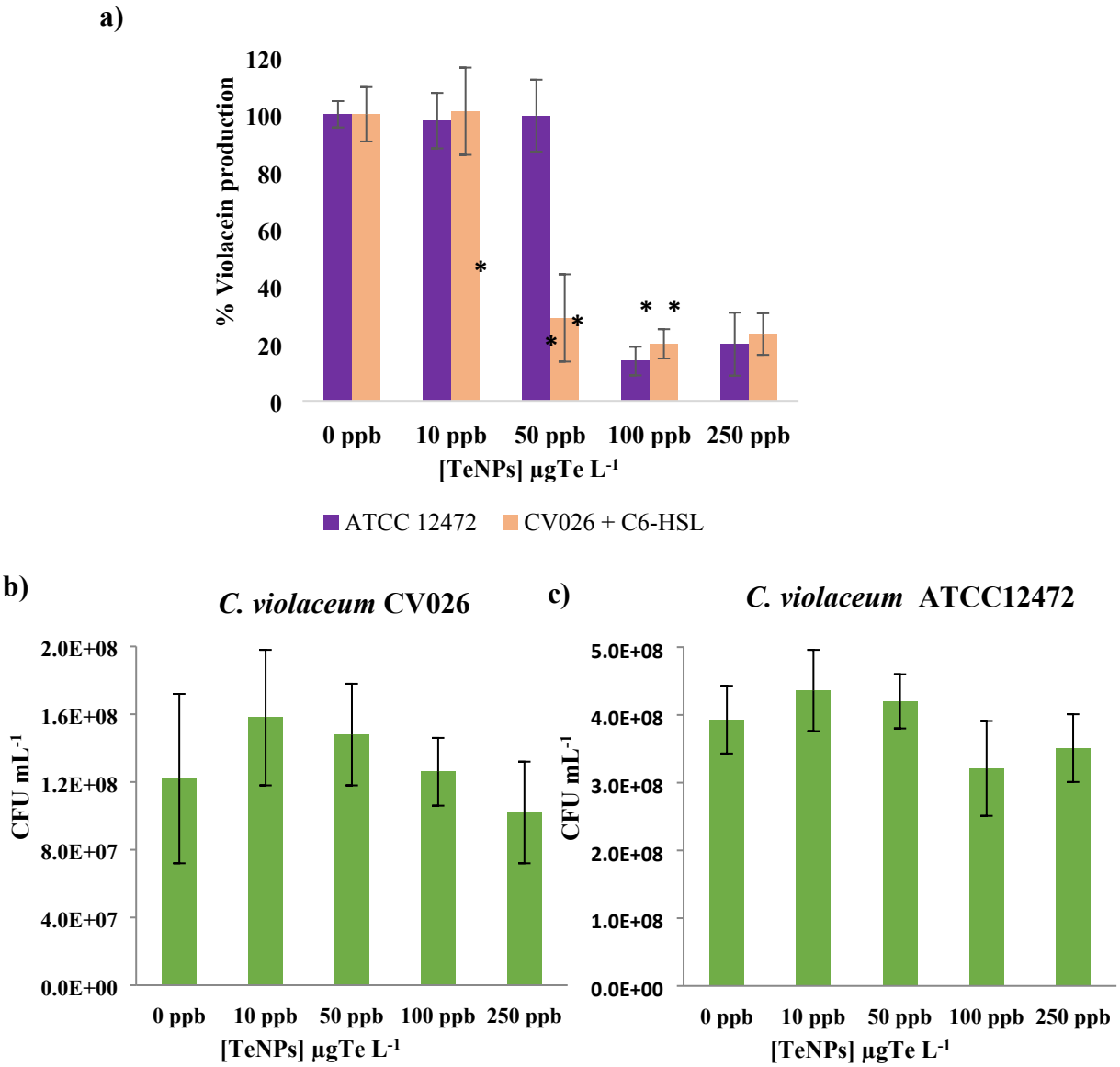

Figure 4.

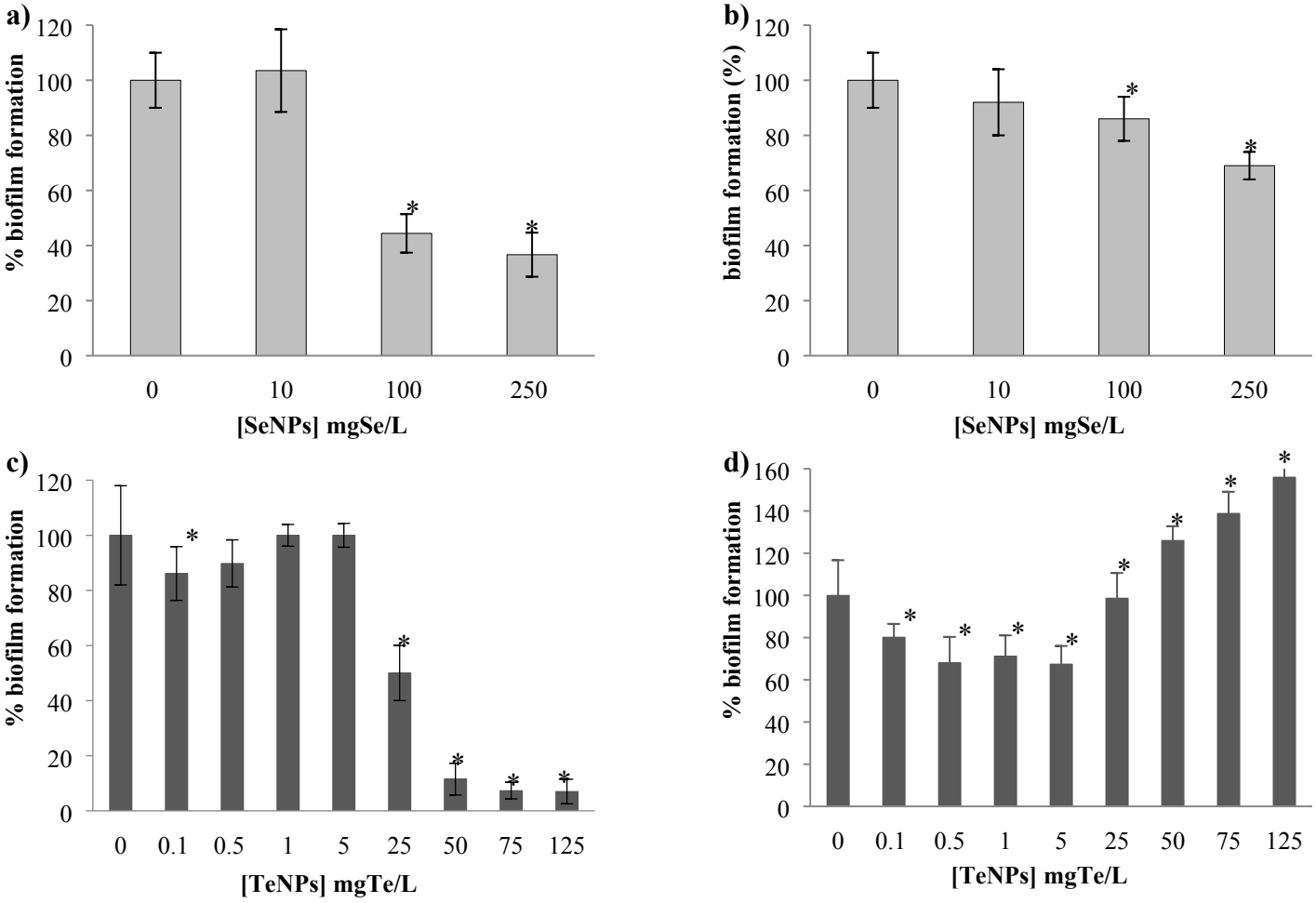

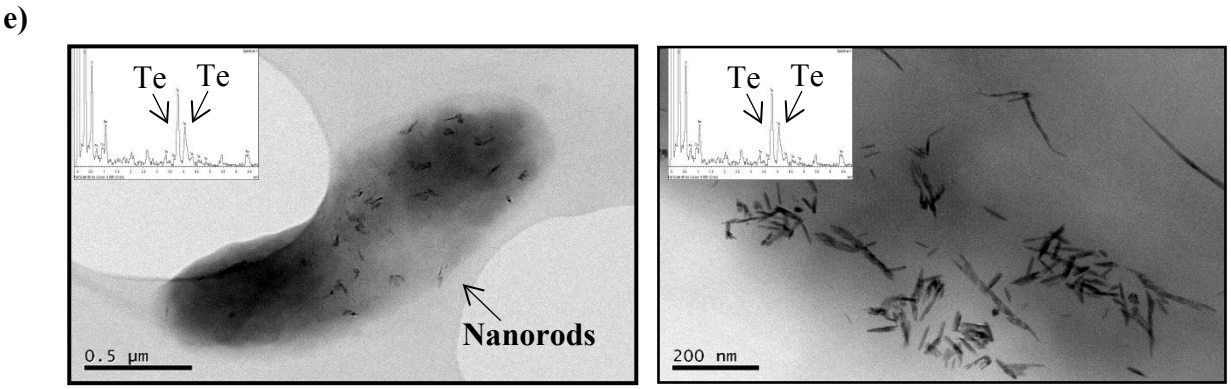

Figure 5

View Article Online
DOI: 10.1039/C9MT00044E

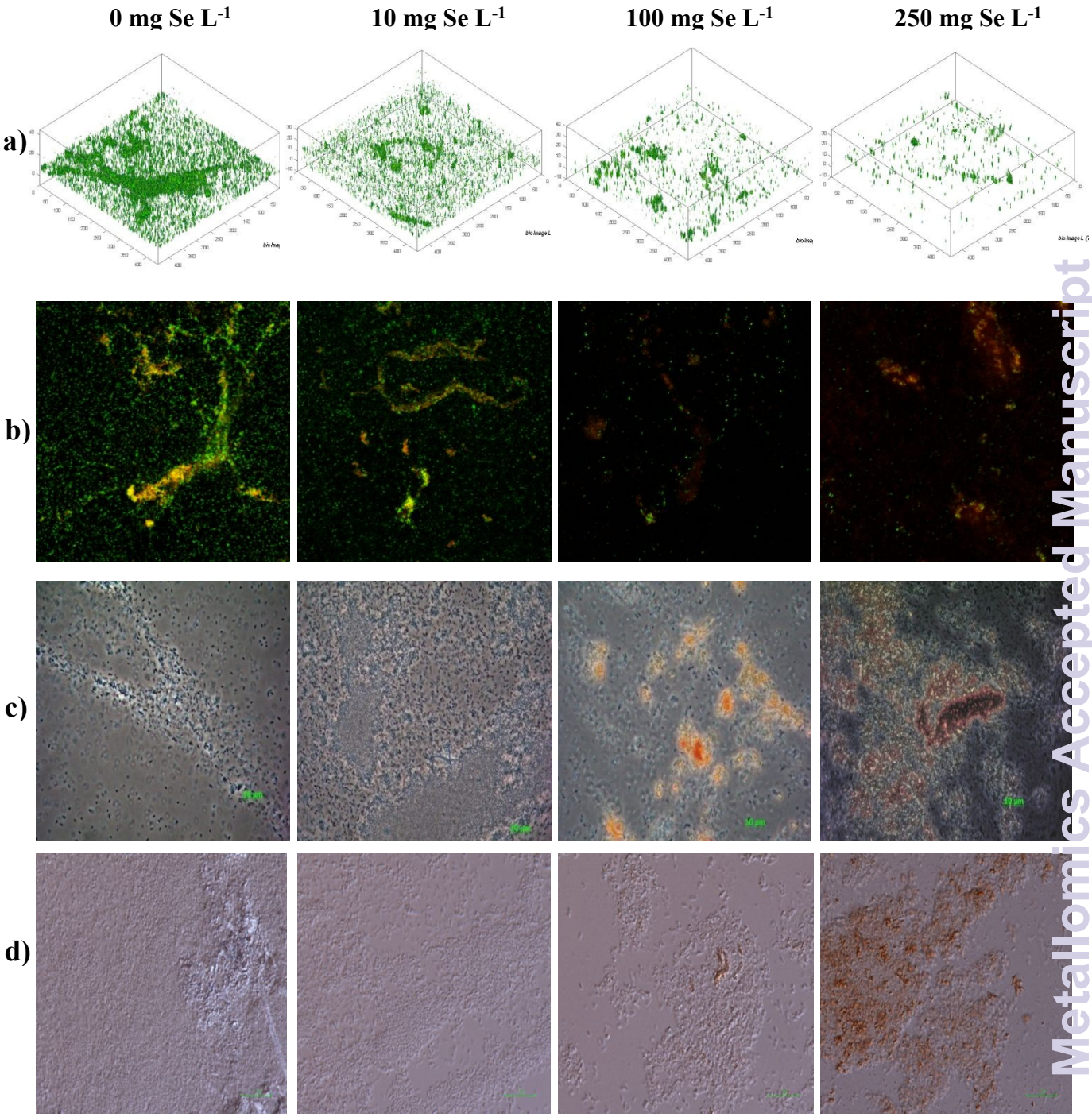

Figure 6

View Article Online
DOI: 10.1039/C9MT00044E